X-ray absorption of $BaBiO_3$ and superconducting $BaBi_{0.25}Pb_{0.75}O_3$

J. B. Boyce
Xerox Palo Alto Research Center, Palo Alto, California 94304

F. G. Bridges
Department of Physics, University of California, Santa Cruz, California 95064

T. Claeson
Physics Department, Chalmers University of Technology, S-41296 Göteborg, Sweden

T. H. Geballe
Department of Applied Physics, Stanford University, Stanford, California 94305

J. M. Remeika*
AT&T Bell Laboratories, Murray Hill, New Jersey 07974

(Received 5 September 1989; revised manuscript received 18 December 1989)

X-ray-absorption studies of $BaBiO_3$ and superconducting $BaBi_{0.25}Pb_{0.75}O_3$ (Ba-Bi-Pb-O) did not show any structural transformations altering the gross-scale near-neighbor environment or the valence between 4 and 300 K. Two Bi-O distances, separated by about 0.17 Å, could be distinguished for $BaBiO_3$. Also in Ba-Bi-Pb-O, there is a strong indication of two different Bi-O distances, separated by about 0.12 Å, but only one Pb-O distance. The differing Bi-O separations may be connected with local spatial charge fluctuations. The valence states of the two differently located Bi atoms could not be conclusively determined from the absorption-edge shape, but the Bi and Pb near-edge structures for Ba-Bi-Pb-O are nearly identical. The Bi-O and Pb-O vibrational frequencies, considered important for superconductivity, could be estimated from the temperature dependence of the broadening of the nearest-neighbor distributions; they correspond to Einstein temperatures of about 500 K.

I. INTRODUCTION

The superconductivity of the perovskite-type oxide $BaBi_xPb_{1-x}O_3$ has acquired renewed interest with the advent of the recent high-temperature superconductors. It may be considered as the archetype of oxide superconductors. The superconducting transition temperature of the $BaBi_{0.25}Pb_{0.75}O_3$ (Ba-Bi-Pb-O) is relatively high[1] ($T_c \approx 11-13$ K) despite the fact that the carrier density and the density of electron states at the Fermi level are much smaller (up to an order of magnitude smaller) than in "ordinary" superconducting metals with similar T_c's. The low density of states and the high T_c imply an exceptionally strong electron-phonon coupling or perhaps another coupling mechanism.[2] The latter possibility has been strengthened by the advent of a new "high-T_c" superconductor,[3] $Ba_{1-x}K_xBiO_3$, which displays transition temperatures as high as 30 K. It would be surprising if the superconductivity in the two differently doped $BaBiO_3$ (Ba-Bi-O) compounds were different in origin.

The new Cu-O superconductors have many similar properties to Ba-Bi-Pb-O, but there are also differences: (i) the structure is similar, i.e., based on layers of distorted perovskite cells; (ii) the optimum T_c is found close to transformations—structural, antiferromagnetic to nonmagnetic or metal to insulator connected with a Peierls transformation caused by the almost perfect nesting of the Fermi surface; (iii) the density of states at the Fermi level and the total number of charge carriers are small; (iv) the doping of the superconducting cuprate oxides is due to substitutions or vacancies at positions outside the 2D CuO_2 planes, while in Ba-Bi-Pb-O it is due to the substitution of Bi for Pb atoms on the conducting paths themselves (in the K-doped $BaBiO_3$, the dopants are located on the Ba sites); (v) the charge transport is two-dimensional (2D) in the copper oxides while it, presumably, is more three-dimensional (3D) in the bismuth oxides.

Several models[2] have been presented in order to explain the superconductivity of Ba-Bi-Pb-O. Band structure calculations by Mattheiss and Hamann[4] stressed the presence of a complex of hybridized O($2p$)-(Pb,Bi)($6s$) states near the Fermi energy, giving a low density of states. These electrons supposedly couple strongly to optical breathing vibration modes occurring between neighboring oxygen and lead-bismuth atoms. Other models[5] stress the remnants of soft phonon modes due to a Peierls-type charge-density-wave instability driven by a perfect nesting Fermi surface or a real space pairing of electrons due to a fluctuating valence on the Bi sites (Bi^{3+} and Bi^{5+} are the common valences for this atom).

The valence of Bi in $BaBiO_3$, as well as in Ba-Bi-Pb-O,

has been a matter of dispute. Two different Bi(1)-O and Bi(2)-O distances identified by neutron diffraction[6,7] supported a difference in the charge density of the two inequivalent sites and a formula $BaBi^{3+}_{0.5}Bi^{5+}_{0.5}O_3$. However, the calculations by Mattheiss and Hamann[4] showed that the charge-density contours surrounding the Bi(1) and Bi(2) sites were almost identical, and an x-ray photoemission spectroscopy (XPS) experiment[8] also indicated a very small charge difference. Recent neutron diffraction experiments by Chaillout *et al.*[9] claimed that the Bi^{3+} and Bi^{5+} cation distribution depends upon the sample preparation and thermal history.

The simple cubic perovskite structure, that is stable at high temperature, gives rise to several composition-dependent distortions at low temperature. The first extensive studies by Cox and Sleight[6] gave an orthorhombic structure for $x<0.05$, a tetragonal one for $0.05<x<0.35$, orthorhombic for $0.35<x<0.9$, and a monoclinic structure at the Bi end of the solution, $x>0.9$. Khan *et al.*[10] concluded from x-ray powder data that the structure is orthorhombic for all compositions. Oda *et al.*[11] examined sintered powder samples and obtained an orthorhombic structure for $0<x<0.9$ and a monoclinic one for $x>0.9$. Single crystals of the superconducting composition, $x=0.25$, showed a structural transformation from an orthorhombic to a monoclinic phase at a temperature of about 160 K. Indications of such a transformation were also obtained from a dielectric anomaly at the same temperature by Bogatko and Venevtsev.[12] A renewed investigation of Oda *et al.*[11] showed that $x=0.25$ compounds could crystallize in either an orthorhombic or a tetragonal phase depending upon flux composition in the melt process. The structural differences between these modifications usually correspond to small changes in the atomic distances, less than or comparable to the spatial resolution of the X-ray Absorption Fine Structure (XAFS) measurements described here.

The superconductivity occurs close to the semimetal-semiconductor transition at about 35 at. % Bi and the T_c is maximum at about 25 at. % Bi. There have been suggestions that the superconductivity is connected with the ordered arrangement of Bi and Pb at the 1:3 composition.[2] However, T_c does not seem to depend upon the structural symmetry to any appreciable extent as it has been possible to synthesize the 25 at. % Bi compound in different structural modifications having roughly[11] the same T_c.

An important question in the understanding of the phenomenon of high-T_c superconductivity is whether the same pairing mechanism applies to both the copper and bismuth oxides. It has been proposed that charge-density waves may be the attractive interaction in the doped $BaBiO_3$ in analogy with the proposed mechanism of spin density waves in the copper-oxide superconductors. The disputed disproportionation of Bi in $BaBiO_3$ would give way to charge-density fluctuations in the doped compound. As it has been proposed that the effective interaction in the copper oxides may be associated with the oxygen atoms rather than the copper atoms, it may then be speculated that the charge distribution on the Bi(Pb)-O bonds plays a more important role for the attractive interaction than the valence fluctuations on Bi itself.[13]

X-ray Absorption Fine Structure (XAFS) measurements are well suited to studying the local environment of absorbing atoms. The number of different neighbor atoms, their separations from the absorbers, and the spread of these distances can be determined. The temperature dependence of the XAFS provides information about distortions or transformations (if they result in changes in the interatomic distances ≥ 0.01 Å) and of the correlated vibrations between pairs of atoms. In some cases, the near-edge structure also yields information on the valence fluctuations or on the bond ligands.

It is the purpose of this work to study the local atomic environment and the atomic vibrations of the Bi and Pb atoms in Ba-Bi-Pb-O and $BaBiO_3$ and to try to correlate the results with the superconductivity properties. Furthermore, we want to compare the findings with those for the new copper-oxide-based superconductors.

II. EXPERIMENTS

Samples of $BaBiO_3$ and $BaBi_{0.25}Pb_{0.75}O_3$ were melted at 1125 °C in a platinum crucible in air and annealed in oxygen at 800 °C as described in Ref. 9. The T_c of the Ba-Bi-Pb-O sample was 10.52–11.02 K. The solidified melt contained large single crystals. These were crushed into powder, mixed with epoxy and molded into thin strips, which were about 2.5 absorption lengths thick. Since T_c may deteriorate due to a loss of oxygen, coarse, medium, and fine powders of the Ba-Bi-Pb-O crystals were used. The strips were mounted in He exchange gas in helium and nitrogen cryostats and investigated between 4.2 and 300 K.

X-ray radiation was supplied by the wiggler beamline IV-1 of the Stanford Synchrotron Radiation Laboratory. Si(111) and Si(220) monochromators were used during different stages of the experiment at low and high photon energies. The Si crystal was tuned off the maximum of the rocking curve to about $\frac{1}{2}$ maximum intensity in order to reduce the harmonic reflections to an acceptable level. The Si(111) crystal was kept at this setting by a feedback loop. Due to excess vibrations of the mount, the Si(220) crystal had to be clamped, leading to an incident intensity varying somewhat with photon energy. Ionization counters with nitrogen or argon gas measured the incident and transmitted radiation intensities. Photographs were taken of the transmitted radiation to ensure the lack of pinholes in the samples.

Data were taken at the Ba K (37.44 keV), the Bi L_{I} (16.385 keV), the Pb L_{III} (13.035 keV), and the Bi L_{III} (13.418 keV) edges. The closeness of the Pb and Bi absorption edges complicated the quantitative analysis since the XAFS at the Pb L_{III} edge interfered with the Bi L_{III} XAFS. A procedure to correct for this interference was developed and is described below.

III. XAFS DATA REDUCTION

The XAFS information was extracted from the absorptance (proportional to the logarithmic ratio of transmit-

ted and incident intensities) by a procedure given in Ref. 14. A slowly varying absorption background was subtracted using the prethreshold absorption. The free atomic absorptance, $\mu^0(\omega)$ in the expression for the absorption cross section, $\mu(\omega)=\mu^0(\omega)[1+\chi(\omega)]$, was then removed using a sixth- or eighth-order polynomial in k ($\hbar^2k^2/2m_e=\hbar\omega-E_{\rm th}$) or several cubic splines, fit from an energy just above the threshold energy, $E_{\rm th}$, to the maximum energy. ($E_{\rm th}$ is the energy at one-half the absorption-edge height.) Hence we could extract the XAFS modulation function, $k\chi(k)$, given by

$$k\chi(k)=\sum_j N_jF_j(k)\sin[2kR_j+\phi_j(k)] \times\exp(-2k^2\sigma_j^2-2R_j/\lambda)/R_j^2 .$$

Here k is the wave vector of the ejected electron, the sum is taken over shells with N_j atoms at distance R_j from the absorbing atom, F_j is the back-scattering amplitude dependent on the kind of atom in shell j, $\phi_j(k)$ is a phase shift depending upon both the scattering and absorbing atoms, λ is the electron mean free path, and σ_j^2 is the mean-square fluctuation of R_j.

The structural parameters (N_j,R_j,σ_j^2) were deduced from the r-space data. Thus the XAFS data were Fourier transformed into real space. A qualitative comparison between the radial distribution of neighbors in different samples can be obtained by inspecting these Fourier transforms (FT) of the XAFS oscillations. However, a more quantitative comparison can be performed by comparing the real and imaginary parts of the FT of $k\chi(k)$ in a certain range of r with identical k space transforms of standards. An iterated minimum of the least-squares difference between the FT of $k\chi(k)$ extracted from the experimental data and that from a model made up from one or several standards gives the amplitude (containing the coordination number), the shift in neighbor separation, and the additional Debye-Waller-type broadening of the pair radial distribution function in question as compared with the signature.[15-17]

IV. THE OXIDATION STATE OF BISMUTH

Bismuth compounds usually have a valence of Bi^{3+}. There also exist some Bi^{5+} compounds, but other valences are rare. Hence it is tempting to consider the Bi in $BaBiO_3$ and Ba-Bi-Pb-O as consisting of a mixture of Bi^{3+} and Bi^{5+} instead of Bi^{4+} (as the chemical formula would imply). Strong initial support for that notion was given by the neutron diffraction results by Cox and Sleight.[6] They showed that the bismuth cations occupied two crystallographically different sites in $BaBiO_3$, giving two Bi-O distances: 2.29 Å and 2.12 Å. The two sites were assigned to Bi^{3+} and Bi^{5+} states, respectively. However, a neutron diffraction study of $BaBiO_3$ by Chaillout *et al.*[18] found nearly equal Bi-O distances for sites Bi(1) and Bi(2); they did not differ more than 0.01 Å. To resolve the discrepancy with the Cox and Sleight[6] experiments, Chaillout *et al.*[9] performed a new, extensive neutron diffraction study of samples annealed differently. That investigation claimed that there was a phase transition at 800–860 °C. Samples quenched from a higher temperature had a random distribution of Bi^{3+} and Bi^{5+}, while those annealed slightly below that temperature displayed a partially ordered arrangement and two different Bi-O distances of about 2.26 and 2.14 Å. The samples we used for our study have been annealed at 800 °C.

There is considerable disagreement in the literature as to the correct valence for Bi in $BaBiO_3$ and Pb substituted materials, and further experimental results are therefore useful. Absorption-edge studies can in principle provide information concerning the Bi valence as the edge position shifts to higher energy as the valence is increased. In Fig. 1 we show the Pb $L_{\rm III}$ and Bi $L_{\rm III}$ absorption edges for PbO, PbO_2, Ba-Bi-Pb-O, $BaBiO_3$, and Bi_2O_3. Several observations and conclusions could be made: (1) No temperature dependence of the near-edge structure is evident for any of the samples in the investigated temperature region of 4–300 K. (2) The Pb $L_{\rm III}$ edge of Ba-Bi-Pb-O is similar to the one for PbO_2; i.e., Pb^{4+} is the oxidation state in Ba-Bi-Pb-O. (3) The Bi $L_{\rm III}$ edge is identical for the fine and coarse powders of Ba-Bi-Pb-O. No gross change was introduced by the fine powdering. (4) The Bi and Pb $L_{\rm III}$ edges of Ba-Bi-Pb-O are very similar, indicating very similar configurations for Pb and Bi and thus an average Bi^{4+} valence. (5) The average energy of the Bi $L_{\rm III}$ edges of Ba-Bi-Pb-O and $BaBiO_3$ are the same. Both are distinctly different from the edge position for Bi_2O_3 (Bi^{3+}) and are consistent with a

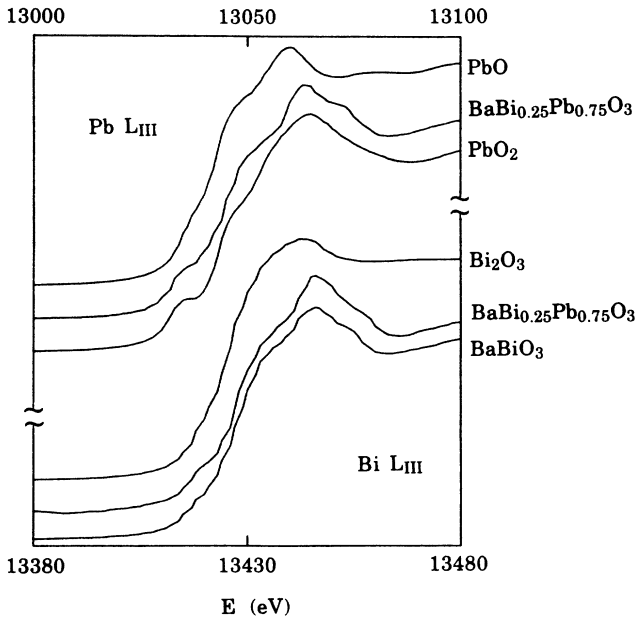

FIG. 1. The Pb $L_{\rm III}$ and Bi $L_{\rm III}$ absorption edges for (from top to bottom) PbO, $BaBi_{0.25}Pb_{0.75}O_3$, PbO_2, Bi_2O_3, $BaBi_{0.25}Pb_{0.75}O_3$, and $BaBiO_3$. Note the resemblance between the Pb and Bi edges for the superconducting sample. There was no change in the data between 4.2 K and room temperature. Toward the low-energy end of the absorption edges there is a weak shoulder, most prominently seen in PbO_2, that is discussed in the text.

Bi^{4+} state.

In summary, the strong similarity between the Bi and Pb edges in Ba-Bi-Pb-O and the same average edge position for Bi in Ba-Bi-Pb-O and $BaBiO_3$ suggest a Bi^{4+} valence. However, the edge data for a Bi^{5+} standard is needed to confirm this assignment.

V. XAFS DATA

In this section we present the XAFS data for the different edges. Figure 2 shows the absorption data at the Pb and Bi L_{III} edges in Ba-Bi-Pb-O and illustrates two features of the data: (1) the good quality in the sense that the signal-to-noise ratio is high, and (2) the problem arising from the closeness of the Pb and Bi L_{III} edges. The XAFS from the Pb L_{III} edge overlaps that from the Bi L_{III} edge and makes detailed comparisons of the Bi environment in the Ba-Bi-Pb-O compound more complicated. The XAFS data, like those in Fig. 2, were reduced, as described in Sec. III.

A. Ba *K* edge XAFS

The Ba K edge XAFS in k space, $k\chi(k)$, for the Ba-Bi-Pb-O sample is shown in Fig. 3, lower curve. Again, the good quality of the data should be noted. Examples of Fourier transforms to r space of the XAFS at the Ba K edge are given in Fig. 4 for Ba-Bi-Pb-O, $BaBiO_3$, and BaO. The expected locations of the different neighbors are also marked; phase shifts have to be added to these distances to coincide with the maxima of the Fourier transform function.

As seen, the oxygen peak is very small in the two samples, Ba-Bi-Pb-O and $BaBiO_3$. There is a strong interference between the O backscatterers at different distances (there are seven first-neighbor Ba-O distances in $BaBiO_3$) as well as from the strong scatterers of Bi(Pb) and Ba that are situated in neighboring shells. Hence, in contrast to Balzarotti *et al.*[19] who investigated the Ba L_{III} edge, we claim that the different Ba-O distances in $BaBiO_3$ cannot be resolved. This is despite the fact that our data on the Ba K edge extend a factor of 2 further in k space and have a good signal-to-noise ratio. The difference between Ba-Bi-Pb-O and $BaBiO_3$ is likely due to different interfer-

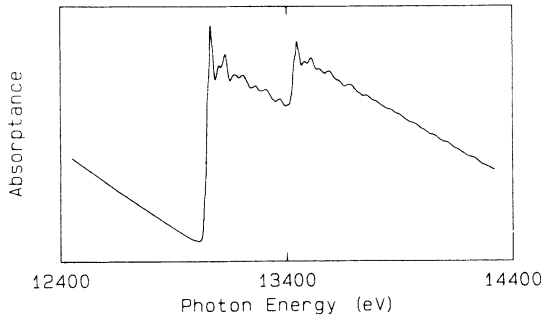

FIG. 2. The x-ray absorption of Ba-Bi-Pb-O in the vicinity of the L_{III} edges of Pb and Bi. The data were taken at 4.2 K with a Si(220) monochromator.

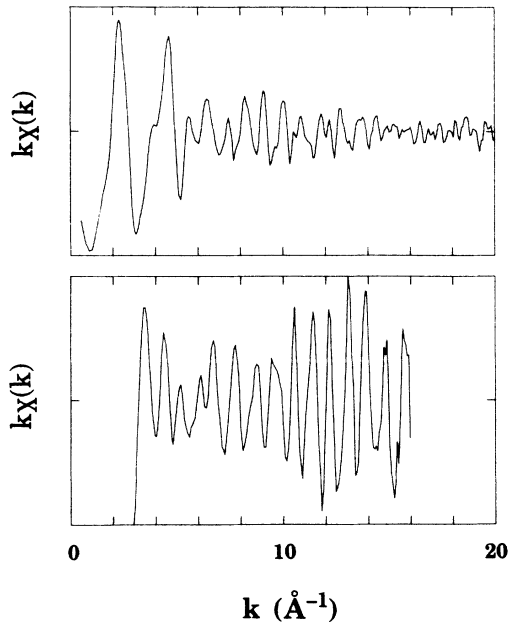

FIG. 3. XAFS at the Ba K edge for $BaBi_{0.25}Pb_{0.75}O_3$ (upper curve) and the Bi L_{III} edge for $BaBiO_3$ (lower curve). The data have been converted to k space and the background has been removed as described in the text using $E_{th}=37\,408$ eV for Ba K and $E_{th}=13\,420$ eV for Bi L_{III}.

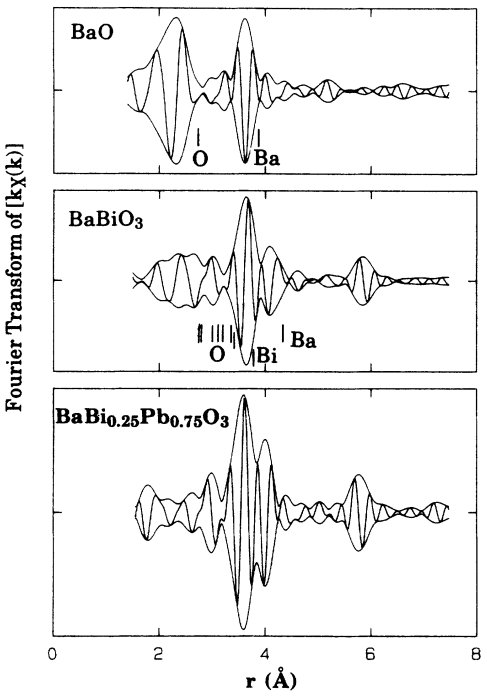

FIG. 4. XAFS at the Ba K edge transformed to r space. Results are shown for BaO, $BaBiO_3$, and $BaBi_{0.25}Pb_{0.75}O_3$, all at 6 K. Both the real part and the absolute value (envelope curve) of the transform are shown. The transform range was 3.2–15.7 $Å^{-1}$, Gaussian broadened by 0.5 $Å^{-1}$. The locations of near neighbors are indicated by bars. Phase shifts have to be added to obtain the actual positions of the neighbor atoms.

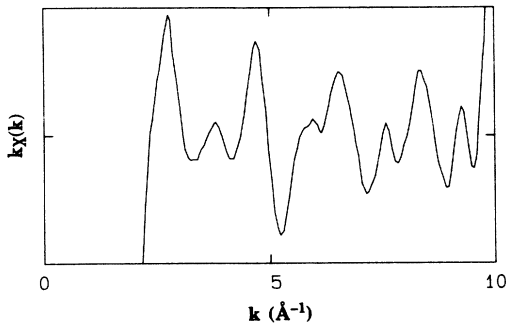

FIG. 5. XAFS at the Pb L_{III} edge for the $BaBi_{0.25}Pb_{0.75}O_3$ sample at $T=4.2$ K. The conversion to k space used $E_{th}=13\,044$ eV.

ences. In contrast, for the structural standard, BaO, the oxygen and barium nearest neighbors are well separated and the corresponding peaks can be resolved with no difficulty, as shown in Fig. 4.

B. Pb L_{III} edge XAFS

An example of the k-space XAFS for the Ba-Bi-Pb-O sample is given in Fig. 5. The XAFS taken with the Si(111) and Si(220) monochromators were identical. The closeness of the Bi L_{III} absorption-edge limits the k range for the Pb L_{III} XAFS to about 9.6 $Å^{-1}$. Hence the Fourier transforms of the Pb $k\chi(k)$ are somewhat broadened. Examples of these are shown in Fig. 6 for the Ba-Bi-Pb-O sample. The structures from the Ba shell at 3.72 Å and from the Pb(Bi) shell at 4.29 Å partly overlap, giving rise to an interference around $r=4.0$ Å. The room temperature XAFS retains the low-temperature shape but exhibits the usual thermal broadening.

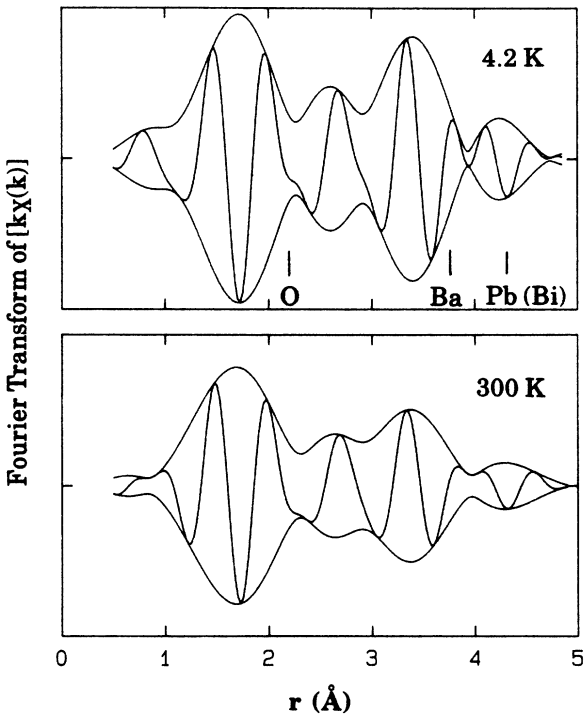

FIG. 6. Pb L_{III} XAFS transformed to r space using a k range of 3.1–9.6 $Å^{-1}$ Gaussian broadened by 0.5 $Å^{-1}$. Both the real part and the absolute value (envelope curve) of the transform are shown. The results for $BaBi_{0.25}Pb_{0.75}O_3$ at two temperatures, 4.2 K and 300 K, are compared. The peak amplitudes at 300 K are depressed by thermal broadening. The locations of neighbors are marked. Vertical scales are the same: ±0.25. Phase shifts have to be added to give the actual positions of the neighboring peaks.

C. Bi L_{III} edge XAFS

The r-space data at the Bi L_{III} edge are presented in Fig. 7 for $BaBiO_3$ and the corresponding k-space data are shown in Fig. 3, upper curve. We have used the same short Fourier transform range in Fig. 7 so that comparisons between $BaBiO_3$ and Ba-Bi-Pb-O can be made. Be-

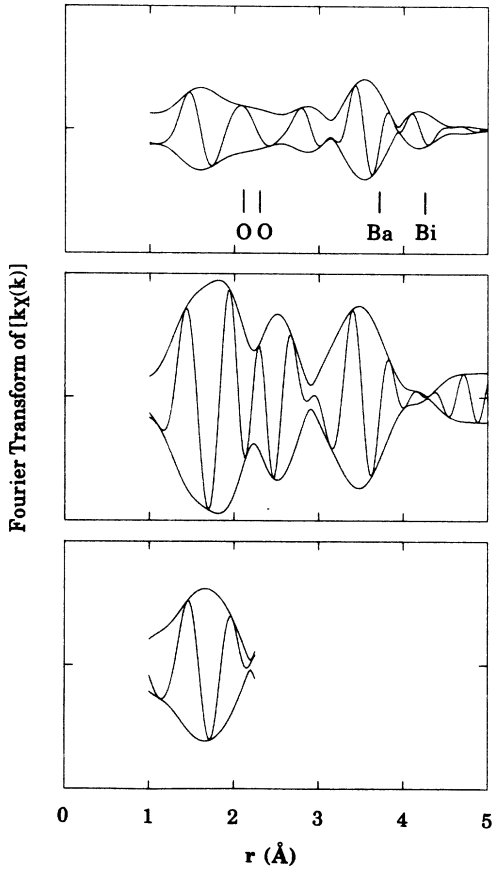

FIG. 7. The Bi L_{III} XAFS transformed to r space for $BaBiO_3$ (top curve) and $BaBi_{0.25}Pb_{0.75}O_3$ (middle). A transform range of 3.6–11.1 $Å^{-1}$ (broadened by 0.3 $Å^{-1}$) was used. Note that the amplitudes, and in particular the one corresponding to the nearest Bi-O distances, are depressed for $BaBiO_3$ due to the destructive interference caused by two Bi-O bond lengths 0.17 Å apart. For the alloy (middle diagram), the Pb L_{III} XAFS gives a sizable background contribution. It is subtracted, as described in the text, to give the resulting nearest-neighbor contribution (Bi-O, bottom diagram) that was used in the subsequent fits. Vertical scales are the same: ±0.5.

cause some of the materials were prepared in a Pt crucible, we were concerned about the possibility of interference from the Pt L edges. A small Pt L_{II} edge of about 1% of the Bi L_{III} edge was observed below the Bi edge. Consequently, the much smaller Pt L_I edge, which occurs at 13.89 keV in the region of the Bi L_{III} XAFS, is too small to influence the data. No evidence for Pt in the Ba-Bi-Pb-O sample was found.

The XAFS at the Bi L_{III} edge for the Ba-Bi-Pb-O is quite similar to the corresponding structure at the Pb L_{III} edge, as can be seen by comparing the Fourier transforms given in Fig. 6. However, the overall amplitude of the Ba-Bi-Pb-O data is too large as a result of the superposition of part of the Pb L_{III} XAFS for $k > 10$ (see Fig. 7). The Pb oscillations for $k > 0$ are shifted in spatial frequency when the Bi L_{III} edge is used for $k = 0$. Roughly speaking, the Pb oscillations for the second and third neighbors produce a background in the vicinity of the Bi-O peak and yet further Pb neighbors produce the background for the Bi second neighbors. To obtain good fits to the standards, we must remove the background; this is difficult to do and has only been carried out for the Bi-O peak as shown in the lower part of Fig. 7. Details of the subtraction are given in the next section.

There is a distinct reduction in the amplitude of the first peak in the $BaBiO_3$ sample as compared to the corresponding peak in the corrected data for Ba-Bi-Pb-O. This is due to the increased destructive interference from two well separated Bi-O distances in $BaBiO_3$ to which we return in the next section. Note that the r-space data itself does not display any split structure due to the small difference in Bi-O separation; this is in contrast to the situation reported in Ref. 19. No substantial changes are seen in the XAFS as the temperature is varied from 4 K to 300 K, aside from a broadening of the peaks.

VI. DETAILED COMPARISONS

To extract numerical results, we performed fits in r space, as described in Sec. III. To detect shifts and broadenings with temperatures, the FT of $k\chi(k)$ for the sample itself at 4 K could be used. However, to obtain the different neighbor distances, independent standards are needed. Thus our first step was to develop good single-peak structural standards. Bi_2O_3 has a complicated crystal structure with several interfering Bi-O distances. For α-PbO_2 the Pb atoms have four O neighbors at 2.167 Å and two at 2.219 Å (at room temperature). This is still quite simple, and so a single-peak Pb-O standard can be constructed from the XAFS of α-PbO_2 by removing the multipeak phase using this known structure, assuming comparable widths for the two components. This procedure is described in Ref. 15. For Bi-O a small correction, using spherical wave calculations,[16] was applied to this Pb-O signature to change the central atom phase from that of Pb ($Z = 82$) to that of Bi ($Z = 83$), as described in Ref. 17. This signature was then used to extract the Bi-O information.

For the (Pb,Bi)-Ba second neighbor standard, the Hg L_{III} data for HgTe was used. An interpolation of the central atom phase for Hg ($Z = 80$) was made to that for Pb or Bi central atoms ($Z = 82$ or 83) using spherical wave calculations. The backscattering phases and amplitudes were obtained in a similar fashion from that of Te ($Z = 52$) to Ba ($Z = 56$). For the third neighbor, a Pb-Pb standard was extracted from fluorite-structured PbF_2; a corresponding Bi-Bi standard was generated from this standard using the spherical wave calculations.[16]

Three types of fits were done.

(1) Analysis of the Pb and Bi L_{III} XAFS for $BaBiO_3$ and Ba-Bi-Pb-O at the different temperatures using the two standards: Pb-O and Bi-O constructed from PbO_2, as described above. We use two-Gaussian fits to determine two different Bi-O (or Pb-O) distances, if present, and compare with one Gaussian fits.

(2) Fits of the second- and third-neighbor shells using Bi-Ba (Pb-Ba) and Bi-Bi (Pb-(Pb,Ba)) standards.

(3) Comparisons of the XAFS at 77 K, 180 K, and 300 K with that at 4.2 K for the same sample. These fits were performed in r space for the regions 1.2–2.0 Å, 3.1–3.8 Å, and 4.1–4.6 Å in order to cover the different neighboring shells. The intention was to see if there occurred any gross structural changes within the region 4–300 K and to study the temperature dependence of the broadenings of the pair correlation functions.

Two different Bi-O distances could be clearly distinguished for the $BaBiO_3$ sample. The separation determined from the fits (about 0.17 Å) is somewhat larger than the one determined by Chaillout *et al.*[9] (0.12 Å) and Thornton and Jacobson[7] (0.12 Å) but agrees well with the value given by Cox and Sleight[6] (0.17 Å). From the separation into two Gaussians it is also possible in principle to extract the Debye-Waller-type broadening for the two distances. We find an indication of different temperature dependencies of the broadening for the two components; however, because of the uncertainty in the extraction of these values (there is some overlap between the longer Bi-O peak and the second neighbors) and the limited number of temperature measurements, we do not emphasize these values at this stage but rather rely upon the one Gaussian fits of the average distribution of Bi-O neighbors to extract vibrational frequencies (see Sec. VII).

The first set of fits to the Bi edge data in Ba-Bi-Pb-O was poor and could not distinguish between a single Bi-O distance and two distances. This is due to the strong contribution from the Pb L_{III} edge XAFS which extends above the Bi L_{III} edge since they are separated by only $\Delta E \approx 383$ eV. The structure is still substantial at the Bi L_{III} edge, and there are three times more Pb atoms than Bi atoms. Hence any fits will be ruined if this contribution is not taken into account. Therefore, we subtracted the Pb contribution from the Bi data. The procedure is as follows: First, a fit to the Pb-edge data including the first three neighbors [Pb-O, Pb-Ba, and Pb-Bi,Pb], using the standards described above, was performed over the allowed k range up to the Bi L_{III} edge, i.e., to $\Delta E \approx 383$ eV or $k \approx 10$ Å^{-1}. The resulting fits gave results that are consistent with what is known about the Pb near-neighbor environment in Ba-Bi-Pb-O and the simulated k-space data fits the Pb data up to $k = 10$ Å^{-1} very well.

Second, these fit results were extended beyond $\Delta E \approx 383$ eV into the Bi-edge region using the longer data range of the structural standards which contain no Bi. These extended fit results were then subtracted from the data. This subtraction removes most of the Pb L_{III} edge data from the Bi region. The result is Bi L_{III} edge data that is relatively free of the Pb L_{III} edge contribution. In actuality, some Pb contribution remains due to three limitations in the procedure: (1) Only the first three Pb-X neighbors were fit, so not all the Pb XAFS is removed. The first three neighbors, however, account for the bulk of the Pb XAFS and provide most of the correction in the vicinity of the Bi-O peak. (2) The Pb standards have a finite k range ($k \approx 16$ Å^{-1}) and so do not extend to a high k value at the Bi edge. Transferred to the Bi edge 383 eV away, this corresponds to $k < 12.5$ Å^{-1} and therefore limits our available transform range in k space. (3) The relative amplitude of the correction depends on the ratio of the number of Pb to number of Bi atoms, i.e., three for the nominal composition. The actual composition can be obtained from the ratio of the step heights at the Pb L_{III} and Bi L_{III} edges. From our edge data, this ratio is about 3.55, corresponding to an actual composition of $BaBi_{0.22}Pb_{0.78}O_3$. This value has some uncertainty due to the XAFS oscillations on both edges. Allowing this ratio parameter to vary in the fits yields a value between 3.8 and 4.0. There is thus some uncertainty in the amplitude of the correction. A value of 3.8 was used for the corrected data shown in the bottom of Fig. 7.

Using this improved procedure, it was, indeed, possible to obtain good fits to the Bi XAFS. Two different Bi-O distances were found for the metallic (superconducting) compound, as for the semiconducting $BaBiO_3$. The fits using two distances gave a root mean-square deviation of the fitted XAFS to the measured one that was a factor of 7 smaller than fits using only one distance. Furthermore, the number of Bi-O neighbors (six O neighbors expected) needed to fit the data (the amplitude of the Gaussian) was more reasonable for the two distance distribution, but the fits indicate that the relative amplitudes of the two peaks are not equal, 3.6 and 2.5, close to a 4-to-2 ratio (see Table I). We cannot determine whether there are two inequivalent Bi sites or an asymmetric distribution of O about the Bi atoms. We assume the latter in assigning the number of neighbors for the alloy. However, we note that a theoretical calculation[20] for alloys of similar composition suggests that two Bi sites might be expected. Two differently prepared samples that were investigated more than two years apart also gave essentially identical distances for the Bi-O separations. Hence we conclude that there are likely two Bi-O distances in the Ba-Bi-Pb-O compound, as in $BaBiO_3$, despite the fact that the extraction procedure in the Ba-Bi-Pb-O case is more complicated. However, because of these complications, we plan to check this result on a series of samples with different Pb concentrations. For the lower Pb concentrations, the corrections will be correspondingly smaller.

The situation for the Pb first neighbor environment is quite different. All fits in Ba-Bi-Pb-O gave only one Pb-O separation of 2.18 Å. The different distances extracted are summarized in Table I.

The errors in the determined values depend upon the complexities of the fits. We have checked for unstable values by changing the starting parameters, the fit ranges, and the transform ranges. The absolute uncertainty in position may be 0.04 Å, but the relative error and variations between different samples are about 0.02 Å. The uncertainties in the number of neighbors are typically

TABLE I. The Bi (Pb) near-neighbor distances and average number of neighbors around the Bi (Pb) sites in $BaBiO_3$ and $BaBi_{0.25}Pb_{0.75}O_3$. A comparison between XAFS and diffraction results is given. The latter are taken from Cox and Sleight (CS, Ref. 6), Thornton and Jacobson (TJ, Ref. 7), Chaillout *et al.* (Cal, Ref. 9), Sleight *et al.* (Sal, Ref. 1), Khan *et al.* (Kal, Ref. 10), and Oda *et al.* (Oal, Ref. 11). The different Bi(1,2)-O(1,2) are grouped together to give average distances for the diffraction data for $BaBiO_3$. For the alloy, all Bi-O and Pb-O distances are taken from average values of the lattice parameters. We give two Bi-O distances for the alloys but cannot determine whether there are two inequivalent Bi sites or an asymmetric distribution of O about the Bi atoms. We assume the latter in assigning the number of neighbors for the alloy. The XAFS and diffraction data were taken at 4 K and 300 K, respectively.

		XAFS		Diffraction			
					r (Å)		
Compound	Pairs	r (Å)	No. of neighbors	CS	TJ	Cal	No. of neighbors
$BaBiO_3$	Bi(1)-O	2.29±0.02	6±1	2.29	2.26	2.26	6
	Bi(2)-O	2.12±0.02	6±1	2.12	2.14	2.14	6
	Bi-Ba	3.75±0.04	8±2	3.77		3.76	8
				Sal	Kal	Oal	
$BaBi_{0.25}Pb_{0.75}O_3$	Bi-O	2.21±0.03	3.6±0.5				
				2.15	2.15	2.14	6
	Bi-O	2.09±0.03	2.5±0.5				
	Pb-O	2.18±0.02	6±1	2.15	2.15	2.14	6
	Pb-Ba	3.68±0.04	10±2	3.72	3.72	3.71	8

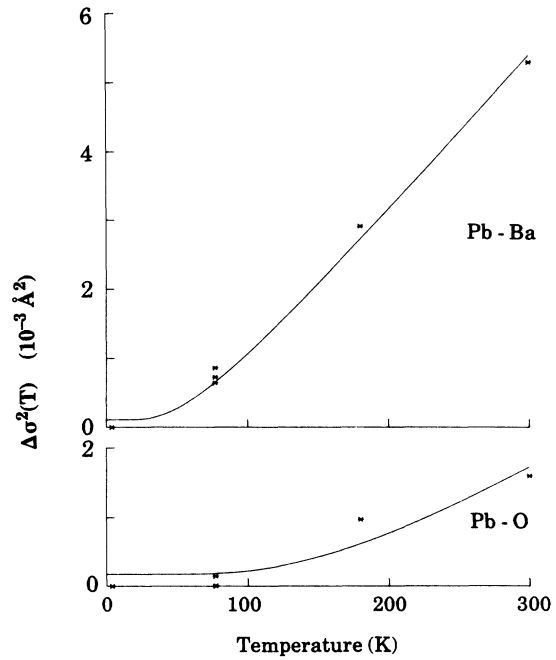

FIG. 8. The Debye-Waller-type factors for the first and second neighbors surrounding absorbing Pb atoms in Ba-Bi-Pb-O relative to the data at 4.2 K. By fitting the temperature dependence of the extra broadening, $\Delta\sigma^2=[\sigma^2(T)-\sigma^2(4\text{ K})]$, it is possible to estimate Einstein temperatures that characterize the pair vibrations (drawn curves are fits). These are $\Theta_E\approx 500$ K for the first Pb-O neighbors and about 130–180 K for the second- and third-neighbor shells. Almost identical results are obtained for the vibrations of Bi-O and Bi further neighbors.

10% but can be as large as 20% in a few cases. The estimated errors are indicated in Table I.

VII. EXTRACTION OF VIBRATIONAL FREQUENCIES

It is possible to estimate the characteristic Einstein vibration frequencies, ω_E, or Einstein temperatures, Θ_E, from the temperature variation of the Debye-Waller-like broadening of the pair distribution function. Assuming that the individual bonds can be treated as Einstein oscillators, one obtains[21]

$$\sigma^2(T)\simeq(\hbar/2\mu\omega_E)\coth(\hbar\omega_E/2k_BT)\ ,$$

where μ is the reduced mass of the pair of atoms. The temperature variation of the spread in neighboring shell distances is shown in Fig. 8 for Pb absorbers in Ba-Bi-Pb-O. Very similar results are obtained for the Bi data. The Debye-Waller-like broadening is considerably smaller for the first shell (Pb-O, Bi-O) than for the further neighbors. From the relative changes in $\sigma^2(T)$ with temperature, it is possible to extract values of the characteristic Einstein temperatures for each of the pairs resolvable in the XAFS spectra:

Θ_E for Pb (or Bi)$-O\approx 500$ K ,

Θ_E for (Pb or Bi)$-$(Ba, Bi, and Pb)≈ 150 K .

These values are of the same order of magnitude as corresponding characteristic temperatures[13,17,22–27] for the high-T_c superconductors La-Sr-Cu-O and Y(Gd)-Ba-Cu-O. Hence the superconductivity is not a function of the stiffness of vibrational modes Pb(Bi)-O or Cu-O. We note that the Einstein temperature that we estimate, 500 K, falls in the same range as the prominent modes[26,27] determined by inelastic neutron scattering and Raman spectroscopy and agrees with the estimates of the breathing mode frequency.

VIII. DISCUSSION AND CONCLUSIONS

No changes that could be related to a gross structural change were seen in either the atomic separation, the Debye-Waller-like broadening, or the near-edge absorption structure as the temperature was varied from 4 to 300 K. The number of temperatures was limited, though, and a small change could have gone unnoticed.

The analysis of the temperature dependence of the broadening of the atom-pair separations, i.e., the Debye-Waller-like factor, disclosed that the Bi (or Pb)-O bonds are the stiffest ones. Considering the Bi(Pb)-O pairs to vibrate as local Einstein oscillators, which probably is a good assumption taking into account the light oxygen mass and the pronounced bond character, we obtained an Einstein temperature of about 500 K. This is considerably higher than the corresponding temperature for the further neighbor mutual vibrations, $\Theta_E\approx 150$ K, which would be more representative of the extended lattice phonons.

We have found similar characteristic temperatures for the Cu-O modes in the high-T_c systems: La_2CuO_4 doped with Ba or Sr, superconducting and semiconducting $YBa_2Cu_3O_y$, and $GdBa_2Cu_3O_y$. They all fall in the range of 400–600 K. There is no correlation between a higher Cu-O (breathing mode) frequency and a higher T_c. In order to explain a high T_c within the electron-phonon context, a high phonon frequency is needed unless the interaction is enhanced by another mechanism. For the Ba-Bi-Pb-O superconductor, these frequencies would suffice, but it is questionable if they are high enough to explain a 100 K superconductor within a nonenhanced, conventional electron-phonon mechanism.

Two separate Bi-O distances were observed in $BaBiO_3$, in good agreement with neutron diffraction results (see Table I). Two Bi-O distances also appear to be present in superconducting $BaBi_{0.25}Pb_{0.75}O_3$. (It should be remarked, though, that this result was found only after a reduction of the background due to the XAFS from the Pb edge and that this procedure adds to the uncertainty in the extracted numbers.) The separations, as well as the two distances themselves, become smaller in the Ba-Bi-Pb-O as expected (the average lattice constant is about 0.07 Å shorter than in $BaBiO_3$). Slightly different distances were obtained in a less rigorous manner from an inspection of the XAFS Fourier transforms in a previous study.[19] Our present detailed analysis of the data shows, however, that fine features in the XAFS may be due to interference between neighboring shells, and that rigorous comparisons with separate standards are needed to obtain numerical values of the distances and number of neigh-

bors.

In the copper oxides, the importance of the O atoms has been stressed. Holes are assumed to be located on O sites rather than on Cu sites. Similarly, it may be that the charge fluctuations are connected with the O atoms in the doped $BaBiO_3$ compound. Or rather one should consider fluctuations connected with the charge distributions of the Bi-O bonds that have a covalent character. These are strongly coupled to atomic separations, i.e., to vibrations. As the Bi content increases, random, localized charge-density fluctuations increase as a result of the two Bi-O distances. At high Bi concentrations, commensurate charge-density waves appear, and a band gap opens up leading to a static distortion and a phase transformation.

The local charge fluctuations may be connected to the local Bi-O octahedra. The Bi-O and Pb-O local environments tend to be the same as those of the end members, at least on the time scale of the XAFS experiment. On the average, Vegard's law is obeyed even if there are local distortions around the Bi and Pb atoms. The situation resembles that of the covalent (Ga,In)As alloys where it has been found that the Ga-As and In-As separations tend to remain almost unchanged upon alloying even if the average lattice constant changes linearly according to Vegard's law.[28]

The situation may be somewhat different for the *K*-doped $BaBiO_3$. In $Ba(Bi,Pb)O_3$, the Bi and Pb have, on the average, the same formal valence and the number of free charge carriers remains small upon alloying. The addition of *K*, on the other hand, leads to a strong doping with holes and the large charge carrier density may quench the charge fluctuations to a large extent. This may explain why the charge-density waves disappear in the strongly *K*-doped alloy.[29]

The apparent local (static or dynamic) variation in the Bi-O distance even in the metallic state is an important concept. It would be of interest to study the transition from the end compound $BaBiO_3$ to the superconductor Ba-Bi-Pb-O and to more securely establish the existence of separate Bi-O and Pb-O distances. Such a study is under way and will be published later.

ACKNOWLEDGMENTS

The experiments were performed at Stanford Synchrotron Radiation Laboratory, which is supported by the U.S. Department of Energy, Office of Basic Sciences, and the National Institutes of Health, Biotechnology Division. This research was supported in part by the U.S. Air Force Office of Scientific Research Grant No. F49620-82CW014 and the Swedish Natural Science Research Council. T.C. would like to thank Xerox Corporation and Stanford University for their hospitality.

*Deceased.

[1]A. W. Sleight, J. L. Gillson, and P. E. Bierstedt, Solid State Commun. **17**, 27 (1975).

[2]For a review of properties, see B. Batlogg, Physica B+C **126B**, 275 (1984); S. Uchida, K. Kitazawa, and S. Tanaka, Phase Transitions **7**, 187 (1986).

[3]L. F. Mattheiss, E. M. Gyorgy, and D. W. Johnson, Jr., Phys. Rev. B **37**, 3745 (1988); R. J. Cava, B. Batlogg, J. J. Kajewski, R. Farrow, L. W. Rupp, Jr., A. E. White, K. Short, W. F. Peck, and T. Kometani, Nature **332**, 814 (1988).

[4]L. F. Mattheiss and D. R. Hamann, Phys. Rev. B **28**, 4227 (1983).

[5]For a review, see E. Jurczek and T. M. Rice, Europhys. Lett. **1**, 225 (1986).

[6]D. E. Cox and A. W. Sleight, Acta Crystallogr. Sect. B **35**, 1 (1979).

[7]G. Thornton and A. J. Jacobson, Acta Crystallogr. Sect. B **34**, 351 (1978).

[8]G. K. Wertheim, J. P. Remeika, and D. N. E. Buchanan, Phys. Rev. B **26**, 2120 (1982).

[9]C. Chaillout, A. Santoro, J. P. Remeika, A. S. Cooper, G. P. Espinosa, and N. Marezio, Solid State Commun. **65**, 363 (1988).

[10]Y. Khan, K. Nahm, M. Rosenberg, and H. Willner, Phys. Status Solidi A **39**, 79 (1977).

[11]M. Oda, Y. Hidaka, A. Katsui, and T. Murakami, Solid State Commun. **55**, 423 (1985); **60**, 897 (1986).

[12]V. V. Bogatko and Yu. N. Venevtsev, Fiz. Tverd. Tela (Leningrad) **25**, 1495 (1983) [Sov. Phys.—Solid State **25**, 859 (1983)].

[13]J. B. Boyce, F. Bridges, T. Claeson, and T. H. Geballe, Phys. Scr. **37**, 912 (1988).

[14]T. M. Hayes and J. B. Boyce, in *Solid State Physics,* edited by H. Ehrenreich, F. Seitz, and D. Turnbull (Academic, New York, 1982), Vol. 37, p. 137.

[15]J. B. Boyce, J. C. Mikkelsen, Jr., F. Bridges, and T. Egami, Phys. Rev. B **33**, 7314 (1986).

[16]A. G. McKale, B. W. Veal, A. P. Paulikas, S.-K. Chan, and G. S. Knapp, J. Am. Chem. Soc. **110**, 3763 (1988).

[17]J. B. Boyce, F. Bridges, T. Claeson, and M. Nygren, Phys. Rev. B **39**, 6555 (1989).

[18]C. Chaillout, J. P. Remeika, A. Santoro, and M. Marezio, Solid State Commun. **56**, 829 (1985).

[19]A. Balzarotti, A. P. Menushenkov, N. Motta, and J. Purans, Solid State Commun. **49**, 887 (1984).

[20]J. O. Sofo, A. A. Aligia, and M. D. Nunez-Regueiro, Phys. Rev. B **39**, 9701 (1989).

[21]E. Sevillano, H. Meuth, and J. J. Rehr, Phys. Rev. B **20**, 4908 (1979).

[22]J. B. Boyce, F. Bridges, T. Claeson, T. H. Geballe, C. W. Chu, and J. M. Tarascon, Phys. Rev. B **35**, 7203 (1987).

[23]J. B. Boyce, F. Bridges, T. Claeson, R. S. Howland, and T. H. Geballe, Phys. Rev. B **36**, 5251 (1987).

[24]C. Y. Yang, S. M. Heald, J. M. Tranquada, A. R. Moodenbaugh, and Y. Xu, Phys. Rev. B **38**, 6568 (1988).

[25]In a preliminary evaluation (Ref. 13) of our results on Bi(Pb)-O vibrations, there was a numerical error giving too high an Einstein temperature.

[26]S. Sugai, Jpn. J. Appl. Phys. **26**, Suppl. **26-3**, 1123 (1987).

[27]W. Reichardt and W. Weber, Jpn. J. Appl. Phys. **26**, Suppl. **26-3**, 1121 (1987).

[28]J. B. Boyce and J. C. Mikkelsen, in *Ternary and Multinary Compounds,* edited by S. K. Deb and A. Zunger (Materials Research Society, Pittsburgh, 1987), p. 359.

[29]S. Pei, N. J. Zaluzec, J. D. Jorgensen, B. Dabrowski, D. G. Hinks, A. W. Mitchell, and D. R. Richards, Phys. Rev. B **39**, 811 (1989).